COMMUNICATIONS IN COMPUTATIONAL PHYSICS
Vol. **5**, No. 2-4, pp. 649-666

Commun. Comput. Phys.
February 2009

Chebyshev Collocation for Optimal Control in a Thermoconvective Flow

M. C. Navarro[1], H. Herrero[1,*] and S. Hoyas[2]

[1] *Departamento de Matemáticas, Facultad de Ciencias Químicas, Universidad de Castilla-La Mancha, 13071 Ciudad Real, Spain.*
[2] *Departamento de Informática, Escuela de Ingeniería, Universidad de Valencia, 46100 Burjassot, Valencia, Spain.*

Received 28 September 2007; Accepted (in revised version) 20 January 2008

Available online 1 August 2008

Abstract. In this paper a Chebyshev collocation method is used for solving numerically an optimal boundary control problem in a thermoconvective fluid flow. The aim of this study is to demonstrate the capabilities of these numerical techniques for handling this kind of problems. As the problem is treated in the primitive variable formulation additional boundary conditions for the pressure and the auxiliary pressure fields are required to avoid spurious modes. A dependence of the convergence of the method on the penalizing parameter that appears in the functional cost is observed. As this parameter approaches zero some singular behaviour in the control function is observed and the order of the method decreases. These singularities are irrelevant in the problem as a regularized control function produces the same results.

AMS subject classifications: 65N35, 76E06, 65K99

Key words: Chebyshev collocation, optimal boundary control, Boussinesq-Navier-Stokes.

1 Introduction

Apart from its appearance in nature, thermoconvective flows occur frequently in industrial applications. For instance, thermoconvective instabilities are responsible for undesirable convective states in some industrial processes such as crystal growth, laser welding or alloy manufacturing [21,22]. In these processes it is important to avoid convective patterns in order to achieve homogeneous and resistant materials. In other words, the control of fluids for the purpose of achieving some desired objective is crucial in those

*Corresponding author. *Email addresses:* `MariaCruz.Navarro@uclm.es` (M. C. Navarro), `Henar.Herrero@uclm.es` (H. Herrero), `sergio.hoyas@uv.es` (S. Hoyas)

applications. In the past, these control problems have been addressed either through expensive experimental processes or through the introduction of significant simplifications into the analysis used in the development of control mechanisms. Recently mathematicians and scientists have been able to address flow control problems in a systematic, rigorous manner and have established a mathematical and numerical foundation for these problems; see [2, 8, 9, 15, 24]. The Chebyshev collocation method is a numerical method broadly used in thermoconvective problems [13, 16, 17]. It has been theoretically studied for fluid dynamics problems [5–7]. But it has not been used in control problems in fluid dynamics because singularities appear in these problems, and spectral methods are less efficient in that case. For this reason finite element approach is the usual method [10, 12].

In this paper, the capabilities of Chebyshev collocation for handling control problems in fluid dynamics will be demonstrated. A Chebyshev collocation method is used to solve numerically a boundary optimal control in a Rayleigh Bénard problem [3, 23] in a cylinder. This problem is extensively described in [18]. The control problem is formulated as a constrained optimization problem, where the constraint is the system of equations that represents steady viscous incompressible Navier-Stokes equations coupled with the energy equation. The choice for the cost is a quadratic functional involving the vorticity in the fluid so that a minimum of that functional corresponds to the minimum possible vorticity subject to the constraints. A linear stability analysis on the controlled states is also performed, so that the convergence tests are performed in terms of the critical values of the bifurcation parameter.

The article is organized as follows. In the second section the convection problem under localized heating is described. The third section explains the optimal control on this problem. The fourth section comprises the numerical results and finally the concluding remarks are summarized in the last section.

2 Formulation of the problem

The physical setup considered consists of a horizontal fluid layer in a cylindrical container of radius l (r coordinate) and depth d (z coordinate). The upper surface is flat and open to the atmosphere where the temperature is T_0. The bottom plate and lateral walls are rigid and the fluid is heated from below by imposing a Gaussian temperature profile which takes the value $T_{\max}$ at $r=0$ and the value $T_{\min}$ at the outer part ($r=l$).

2.1 Equations

The system evolves according to the momentum and mass balance equations and to the energy conservation principle. We concentrate on the study of stationary solutions and, in this sense, the stationary problem is considered. In the equations that govern the system, u_x, u_y and u_z are the components of the velocity field $\mathbf{u}$ of the fluid, T the temperature, p the pressure and $\mathbf{x}=(x,y,z)$ are the spatial coordinates. The governing dimensionless steady state equations are the continuity equation

$$\nabla\cdot\mathbf{u}=0, \tag{2.1}$$

the energy balance equation

$$\mathbf{u}\cdot\nabla\Theta=\nabla^2\Theta, \tag{2.2}$$

and the Navier-Stokes equations

$$(\mathbf{u}\cdot\nabla)\mathbf{u}=\mathrm{Pr}\left(-\nabla p+\nabla^2\mathbf{u}+\mathrm{R}\Theta\mathbf{e}_z\right), \tag{2.3}$$

where $\mathbf{e}_z$ is the unitary vector in the vertical direction, Pr is the Prandtl number and R the Rayleigh number, which is representative of the buoyancy effect and is the bifurcation parameter (see [18]). Here the Oberbeck-Boussinesq approximation has been used (see [13]). The domain, after introducing the dimensionless form, transforms into the cylinder Ω of radius γ and depth 1, where $\gamma=l/d$.

2.2 Boundary conditions

Let us define the boundaries $\Gamma_0=\{(x,y,z)\in\mathbb{R}^3:0<z<1,\ x^2+y^2=\gamma^2\}$,$\Gamma_1=\{(x,y,z)\in\mathbb{R}^3: x^2+y^2\le\gamma^2,z=1\}$ and $\Gamma_2=\{(x,y,z)\in\mathbb{R}^3:x^2+y^2\le\gamma^2,z=0\}$, and $\partial\Omega=\Gamma=\Gamma_0\cup\Gamma_1\cup\Gamma_2$. The top surface is flat and free slip, which implies the following conditions on the velocity,

$$u_z=0,\ \text{on}\,\Gamma_1,\quad \partial_z u_x=\partial_z u_y=0,\ \text{on}\,\Gamma_1. \tag{2.4}$$

The lateral and bottom walls are rigid, so

$$u_x=u_y=u_z=0\ \ \text{on}\ \Gamma_i,\quad i=0,2. \tag{2.5}$$

The lateral wall is considered to be insulating,

$$\partial_n\Theta=0,\ \ \text{on}\ \Gamma_0, \tag{2.6}$$

where ∂_n represents the normal derivative. A heat exchange on the upper surface is considered,

$$\partial_z\Theta=-B\Theta,\ \ \text{on}\ \Gamma_1, \tag{2.7}$$

where B is the Biot number. At the bottom a Gaussian profile for temperature is imposed (see Fig. 1),

$$\Theta(x,y)=\Theta_1(r)=1-\delta\Big(e^{(\frac{1}{\beta})^2}-e^{(\frac{1}{\beta}-(\frac{r}{\gamma})^2\frac{1}{\beta})^2}\Big)/\Big(e^{(\frac{1}{\beta})^2}-1\Big)\ \text{on}\ \Gamma_2, \tag{2.8}$$

where $r=\sqrt{x^2+y^2}$, $\delta=\Delta T_h/\Delta T_v$, $\Delta T_h=T_{\max}-T_{\min}$, $\Delta T_v=T_{\max}-T_0$ and β is a parameter that measures the sharpness of the Gaussian profile.

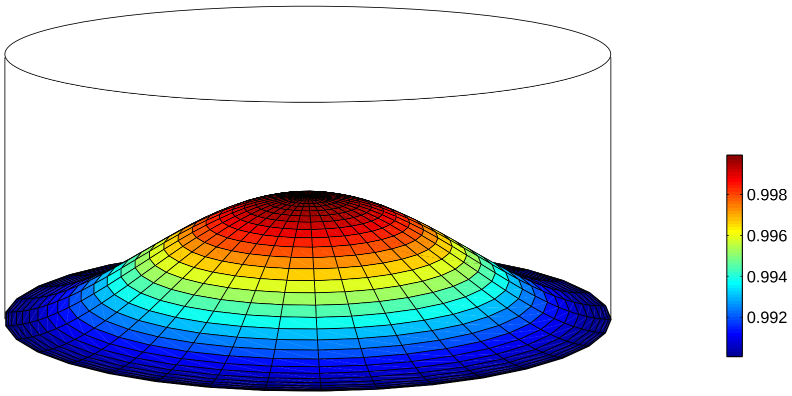

Figure 1: $3D$ plot of the thermal boundary condition Θ_1 at the bottom of the cylindrical domain. The parameters are $B=0.05$, $\gamma=10$, $\mathrm{Pr}=0.4$, $\mathrm{R}=14736$, $\delta=0.01$, and $\beta=5$.

2.3 Stationary solutions

The existence of time-independent solutions to the stationary problem obtained from Eqs. (2.1)-(2.8) is proved in [1]. An example of this type of solution can be seen in Fig. 2 where contour plots for the fields are shown. This basic state bifurcates to a spiral pattern by increasing the Rayleigh number (see [18]).

3 Optimal control problem

If we consider the vorticity of the flow $\omega=\nabla\times\mathbf{u}$, which is a vector related to the local rotation in the fluid flow, and a measure of it, $E(\mathbf{u})=\int_\Omega|\nabla\times\mathbf{u}|^2 d\Omega$, which is called enstrophy. The appearance of patterns is accompanied by an increase of the enstrophy in the flow [19]. This suggests that by reducing the enstrophy we could obtain states for which patterns will also be reduced. For this reason we state the following optimal control problem by looking for the temperature control function h on the top boundary which minimizes the enstrophy of the flow:

Minimize

$$J(\mathbf{u},h)=\frac{1}{2}\int_\Omega|\nabla\times\mathbf{u}|^2 d\Omega+\frac{\eta}{2}\int_{\Gamma_1}h^2 d\Gamma,$$

subject to the state

$$\nabla\cdot\mathbf{u}=0, \tag{3.1}$$

$$\mathbf{u}\cdot\nabla\Theta-\Delta\Theta=0, \tag{3.2}$$

$$(\mathbf{u}\cdot\nabla)\mathbf{u}+\mathrm{Pr}(\nabla p-\Delta\mathbf{u}-\mathrm{R}\Theta\mathbf{e}_z)=0, \tag{3.3}$$

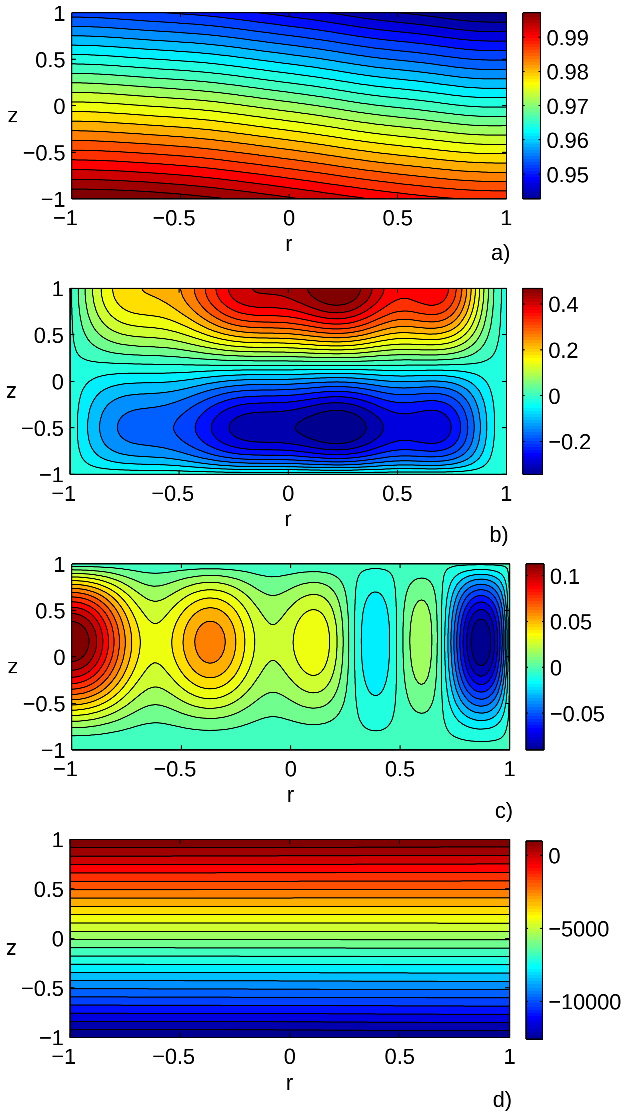

Figure 2: Contour plots for the fields of the uncontrolled basic state; a) Θ; b) u_r; c) u_z; d) p. The parameters are $B=0.05$, $\gamma=10$, $\mathrm{Pr}=0.4$, $\mathrm{R}=14736$, $\delta=0.01$ and $\beta=5$.

with the boundary conditions as follows:

$$\mathbf{u}=0, \quad \partial_n\Theta=0 \ \text{ on } \Gamma_0, \tag{3.4}$$

$$\partial_n u_x=0, \quad \partial_n u_y=0, u_z=0, \quad \partial_n\Theta=Bh-B\Theta \ \text{ on } \Gamma_1, \tag{3.5}$$

$$\mathbf{u}=0, \quad \Theta=\Theta_1 \ \text{ on } \Gamma_2. \tag{3.6}$$

In the cost functional J, the term $\int_{\Gamma_1} h^2 d\Gamma$ is the measure of the magnitude of the control and the penalizing parameter η adjusts the size of the terms in the cost $(0<\eta<\infty)$. The existence of an optimal control for the weak formulation of this control problem is proved in [1].

3.1 Optimality conditions

The following optimality conditions are found in [1]:

$$\nabla\cdot\mathbf{u}=0, \tag{3.7}$$

$$\mathbf{u}\cdot\nabla\Theta=\Delta\Theta, \tag{3.8}$$

$$(\mathbf{u}\cdot\nabla)\mathbf{u}=\mathrm{Pr}(-\nabla p+\Delta\mathbf{u}+\mathrm{R}\Theta e_z), \tag{3.9}$$

$$\nabla\cdot\boldsymbol{\xi}=0, \tag{3.10}$$

$$-\mathbf{u}\cdot\nabla\lambda=\Delta\lambda+\mathrm{PrR}\boldsymbol{\xi}e_z, \tag{3.11}$$

$$-(\mathbf{u}\cdot\nabla)\boldsymbol{\xi}+(\nabla\mathbf{u})^t\boldsymbol{\xi}=\mathrm{Pr}(-\nabla\pi+\Delta\boldsymbol{\xi})-\lambda\nabla\Theta-(\nabla\times(\nabla\times\mathbf{u})), \tag{3.12}$$

together with the boundary conditions

$$\mathbf{u}=0,\quad \partial_n\Theta=0,\quad \boldsymbol{\xi}=0,\quad \partial_n\lambda=0 \ \text{ on } \Gamma_0, \tag{3.13a}$$

$$\partial_n u_x=\partial_n u_y=0,\quad u_z=0,\quad \partial_n\Theta=Bh-B\Theta \ \text{ on } \Gamma_1, \tag{3.13b}$$

$$\partial_n\xi_x=,\quad \partial_n\xi_y=0,\quad \xi_z=0,\quad \partial_n\lambda=-B\lambda,\quad B\lambda-\eta h=0 \ \text{ on } \Gamma_1, \tag{3.13c}$$

$$\mathbf{u}=0,\quad \Theta=\Theta_1,\quad \boldsymbol{\xi}=0,\quad \lambda=0 \ \text{ on } \Gamma_2, \tag{3.13d}$$

where ξ, λ and π are the auxiliary fields.

3.2 Numerical method

Due to the numerical treatment of the problem additional boundary conditions for pressure p and adjoint pressure π are introduced according to [11], i.e. the continuity equation on $z=0$, the normal component of momentum equation on $r=\gamma$, and the normal component of momentum equation on $z=1$. The domain is a cylinder, so a change to cylindrical coordinates is required to simplify the numerical calculation and regularity conditions on $r=0$ have to be introduced,

$$u_r=u_\phi=u_z=\xi_r=\xi_\phi=\xi_z=0,\quad \partial_r\Theta=\partial_r\lambda=\partial_r p=\partial_r\pi=0. \tag{3.14}$$

An iterative procedure as a Newton method is developed in order to handle the nonlinearities. Each linear system is solved with a Chebyshev collocation method, then a change to $[\bar{r},\bar{z}]\in[-1,1]\times[-1,1]$ is required as well. In the following the bars have been eliminated to simplify notation. The basic state is considered to be axisymmetric and therefore depends only on r-z coordinates (i.e., all ϕ derivatives are zero). This kind of assumption makes sense due to the fact that axisymmetric solutions are found in experiments [14]. Equations and boundary conditions after these changes and assumptions become as follows:

$$Gu_r + A\partial_r u_r + 2\partial_z u_z = 0, \tag{3.15a}$$

$$Au_r\partial_r\Theta + 2u_z\partial_z\Theta = \Delta_b\Theta, \tag{3.15b}$$

$$\mathrm{Pr}^{-1}(Au_r\partial_r u_r + 2u_z\partial_z u_r - Gu_\phi^2) = -A\partial_r p + \Delta_b u_r - G^2 u_r, \tag{3.15c}$$

$$\mathrm{Pr}^{-1}(Au_r\partial_r u_\phi + 2u_z\partial_z u_\phi + Gu_r u_\phi) = \Delta_b u_\phi - G^2 u_\phi, \tag{3.15d}$$

$$\mathrm{Pr}^{-1}(Au_r\partial_r u_z + 2u_z\partial_z u_z) = -2\partial_z p + \Delta_b u_z + \mathrm{R}\Theta, \tag{3.15e}$$

$$G\xi_r + A\partial_r\xi_r + 2\partial_z\xi_z = 0, \tag{3.15f}$$

$$-Au_r\partial_r\lambda - 2u_z\partial_z\lambda - \mathrm{PrR}\xi_z = \Delta_b\lambda, \tag{3.15g}$$

$$\begin{aligned}&\mathrm{Pr}^{-1}(-Au_r\partial_r\xi_r - 2u_z\partial_z\xi_r + Gu_\phi\xi_\phi + A\xi_r\partial_r u_r + A\xi_\phi\partial_r u_\phi + A\xi_z\partial_r u_z)\\ &\quad = -A\partial_r\pi + \Delta_b\xi_r - G^2\xi_r + \mathrm{Pr}^{-1}(4\partial_z^2 u_r - 2A\partial_r\partial_z u_z - A\lambda\partial_r\Theta),\end{aligned} \tag{3.15h}$$

$$\begin{aligned}&\mathrm{Pr}^{-1}(-G\xi_r u_\phi + Gu_r\xi_\phi - A^2\partial_r^2 u_\phi + G^2 u_\phi - AG\partial_r u_\phi)\\ &\quad = \Delta_b\xi_\phi - G^2\xi_\phi + 4\mathrm{Pr}^{-1}\partial_z^2 u_\phi,\end{aligned} \tag{3.15i}$$

$$\begin{aligned}&\mathrm{Pr}^{-1}(-Au_r\partial_r\xi_z - 2u_z\partial_z\xi_z + 2G\partial_z u_r - AG\partial_r u_z + 2\xi_r\partial_z u_r + 2\xi_\phi\partial_z u_\phi + 2\xi_z\partial_z u_z)\\ &\quad = -2\partial_z\pi + \Delta_b\xi_z + \mathrm{Pr}^{-1}(A^2\partial_r^2 u_z - 2A\partial_r\partial_z u_r - 2\lambda\partial_z\Theta),\end{aligned} \tag{3.15j}$$

$$\mathbf{u} = 0, \quad \partial_r\Theta = 0, \quad \boldsymbol{\xi} = 0, \quad \partial_r\lambda = 0 \ \text{ on } r = 1, \tag{3.16a}$$

$$u_r = u_\phi = \partial_r u_z = \partial_r\Theta = 0, \quad \xi_r = \xi_\phi = \partial_r\xi_z = \partial_r\lambda = 0 \ \text{ on } r = -1, \tag{3.16b}$$

$$\mathbf{u} = 0, \quad \Theta = \Theta_1, \quad \boldsymbol{\xi} = 0, \quad \lambda = 0 \ \text{ on } z = -1, \tag{3.16c}$$

$$\partial_z u_r = \partial_z u_\phi = 0, \quad u_z = 0, \quad 2\partial_z\Theta = Bh - B\Theta \ \text{ on } z = 1, \tag{3.16d}$$

$$\partial_z\xi_r = \partial_z\xi_\phi = 0, \quad \xi_z = 0, \quad 2\partial_z\lambda = -B\lambda, \quad B\lambda - \eta h = 0 \ \text{ on } z = 1, \tag{3.16e}$$

where

$$G(r) = \frac{2}{\gamma(1+r)}, \quad A = \frac{2}{\gamma}, \quad \Delta_b = A^2\partial_{rr}^2 + GA\partial_r + 4\partial_{zz}^2.$$

3.2.1 Nonlinearities

We have solved numerically the problem (3.15)-(3.16) by treating the nonlinearities appearing in the equations with a Newton-like iterative method. After the changes of variables and with the axisymmetry assumption the domain is transformed into $\tilde{\Omega} = (-1,1)\times(-1,1)$. Let us consider the operator $\mathcal{G}: D(\mathcal{G}) \to L^2\left(\tilde{\Omega}\right)^{10} \times L^2(-1,1)$ defined by Eqs. (3.15)-(3.16) where $D(\mathcal{G})$ is the domain of $\mathcal{G}$ and $L^2(-1,1)$ refers to the image of the h equation in (3.16e). The problem can be rewritten in the following form: To find $U^b \in D(\mathcal{G})$ such that

$$\mathcal{G}\left(U^b\right) = \mathbf{0}, \tag{3.17}$$

where $U^b = (u_r^b, u_\phi^b, u_z^b, \Theta^b, p^b, \xi_r^b, \xi_\phi^b, \xi_z^b, \lambda^b, \pi^b, h^b)$. The operator $\mathcal{G}$ can be broken down in two parts as follows

$$\mathcal{G}U^b := \mathcal{L}U^b + \mathcal{N}U^b,$$

where $\mathcal{L}$ corresponds to the linear part and $\mathcal{N}$ to the nonlinear part. Starting with an initial approximation U^0 and solving the linearized problem around the previous step U^i a classical Newton procedure is defined by

$$\mathcal{L}\bar{U}^{i+1}+\mathcal{N}'\left(U^i\right)\bar{U}^{i+1}=-\mathcal{G}U^i, \tag{3.18}$$

where $\bar{U}^{i+1}=U^{i+1}-U^i$ and $\mathcal{N}'$ is the Fréchet derivative of $\mathcal{N}$. The convergence criterion considered to stop the iterative procedure is that the l^2 norm of the computed perturbation $U=U^{i+1}-U^i$ should be less than certain tolerance v

$$\left\|\bar{U}^{i+1}\right\|_2=\left\|U^{i+1}-U^i\right\|_2\le v,$$

where v is taken of order 10^{-9}.

3.2.2 Chebyshev collocation method

This is a numerical method often used in thermoconvective problems [13, 17] which has been demonstrated to be an efficient and useful tool for solving numerically the partial differential equations that model those problems. Regarding to the theoretical aspects, the convergence of the collocation method can be proved in simpler problems, such as Stokes with Dirichlet boundary conditions or mixed Dirichlet-Neumann problems [4]. But the theoretical treatment with weighted Sobolev spaces (as for Chebyshev collocation) increases the difficulties [4–6] and it can not be proved for Neumann conditions. Then for the problem considered in here, Navier-Stokes equations coupled with heat equation and mixed boundary conditions, only a numerical study of the convergence of the method will be performed. Moreover, this method has already been validated with test problems [11].

3.2.3 Practical implementation

Let us define the boundaries of the domain $\tilde{\Omega}$ as follows

$$\tilde{\Gamma}_0=\{(r,z)\in\mathbb{R}^2:-1\le z\le 1,\ r=1\},\quad \tilde{\Gamma}_1=\{(r,z)\in\mathbb{R}^2:-1<r<1,\ z=1\},$$
$$\tilde{\Gamma}_2=\{(r,z)\in\mathbb{R}^2:-1<r<1,\ z=-1\},\quad \tilde{\Gamma}_3=\{(r,z)\in\mathbb{R}^2:-1\le z\le 1,\ r=-1\}$$

and $\partial\tilde{\Omega}=\tilde{\Gamma}=\tilde{\Gamma}_0\cup\tilde{\Gamma}_1\cup\tilde{\Gamma}_2\cup\tilde{\Gamma}_3$. We define the space $X^{nm}=(\mathbb{P}^{nm}(\tilde{\Omega}))^{10}\times\mathbb{P}^n(\tilde{\Omega})$, where $\mathbb{P}^{nm}(\tilde{\Omega})$ is the space of polynomials of degree n in the r component and m in the z component and $\mathbb{P}^n(\tilde{\Omega})$ is the space of polynomials of degree n in the r component. X^{nm} is the space in which the approximation to the solution of the problem will be sought. The set of Chebyshev polynomials $\mathcal{B}=\left\{T_i(r)T_j(z)\right\}_{0\le i\le n,0\le j\le m}$ form an orthogonal basis of $\mathbb{P}^{nm}(\tilde{\Omega})$ on $[-1,1]\times[-1,1]$ with the scalar product defined continuously as

$$(u,v)_\omega=\int_{\tilde{\Omega}}uv\omega d\tilde{\Omega},$$

where ω is the Chebyshev weight $\omega=(1-r^2)^{-1/2}(1-z^2)^{-1/2}$. We approximate the solution U by an element of X^{nm}, $U(r,z)\sim U^{nm}(r,z)$. Each field of U^{nm} can be expanded in $\mathcal{B}$ as follows

$$w^{nm}=\sum_{i=0}^{n}\sum_{j=0}^{m}a_{ij}^{w}T_i(r)T_j(z), \tag{3.19}$$

where w refers to the unknown fields u_r, u_ϕ, u_z, p, Θ, ξ_r, ξ_ϕ, ξ_z, π and λ. For h only in one dimension is considered.

$$h=\sum_{i=0}^{n}a_i^h T_i(r). \tag{3.20}$$

We then follow the following scheme:

• Define the Chebyshev-Gauss-Lobatto collocation points given by

$$r_i=-\cos\frac{\pi i}{n},\quad z_j=-\cos\frac{\pi j}{m},\quad 0\le i\le n \text{ and } 0\le j\le m$$

and the corresponding two dimensional grid

$$\Xi=\left\{\left(r_i,z_j\right),\, i=0,\cdots,n,\, j=0,\cdots,m\right\}.$$

• Substitute expansions (3.19) for U^{nm} into equations (3.15) and evaluate them at the inner points of the grid:

$$\mathcal{L}U^{nm}(\mathbf{r})+\mathcal{N}'\left(U^{i^{nm}}(\mathbf{r})\right)U^{nm}(\mathbf{r})=-\mathcal{G}U^{i^{nm}}(\mathbf{r}),\quad \mathbf{r}\in\Xi\cap\tilde{\Omega},$$

where $U^{i^{nm}}$ is the approximation to U^b obtained at the previous step i. Consequently, $10(n-1)(m-1)$ linear independent equations are obtained.

• Evaluate the boundary conditions at $r=-1$ for the nodes z_j, $j=0,\cdots,m$,

$$\begin{aligned}&\mathbf{u}^{nm}(\mathbf{r})=-\mathbf{u}^{i^{nm}}(\mathbf{r}),\quad \partial_r\Theta^{nm}(\mathbf{r})=-\partial_r\Theta^{i^{nm}}(\mathbf{r}),\quad \partial_r p^{nm}(\mathbf{r})=-\partial_r p^{i^{nm}}(\mathbf{r}),\ \mathbf{r}\in\Xi\cap\tilde{\Gamma}_3,\\&\boldsymbol{\xi}^{nm}(\mathbf{r})=-\boldsymbol{\xi}^{i^{nm}}(\mathbf{r}),\quad \partial_r\lambda^{nm}(\mathbf{r})=-\partial_r\lambda^{i^{nm}}(\mathbf{r}),\quad \partial_r\pi^{nm}(\mathbf{r})=-\partial_r\pi^{i^{nm}}(\mathbf{r}),\ \mathbf{r}\in\Xi\cap\tilde{\Gamma}_3.\end{aligned}$$

These are $10(m+1)$ equations.

• Evaluate the boundary conditions at $r=1$ for the nodes z_j, $j=0,\cdots,m$,

$$\begin{aligned}&\mathbf{u}^{nm}(\mathbf{r})=-\mathbf{u}^{i^{nm}}(\mathbf{r}),\ \partial_r\Theta^{nm}(\mathbf{r})=-\partial_r\Theta^{i^{nm}}(\mathbf{r}),\quad \mathbf{r}\in\Xi\cap\tilde{\Gamma}_0,\\&\boldsymbol{\xi}^{nm}(\mathbf{r})=-\boldsymbol{\xi}^{i^{nm}}(\mathbf{r}),\ \partial_r\lambda^{nm}(\mathbf{r})=-\partial_r\lambda^{i^{nm}}(\mathbf{r}),\quad \mathbf{r}\in\Xi\cap\tilde{\Gamma}_0.\end{aligned}$$

Consequently, $8(m+1)$ equations are obtained.

• Evaluate the boundary conditions at $z=-1$ for the nodes r_i, $i=1,\cdots,n-1$,

$$\begin{aligned}&\mathbf{u}^{nm}(\mathbf{r})=-\mathbf{u}^{i^{nm}}(\mathbf{r}),\ \Theta^{nm}(\mathbf{r})=\tilde{\Theta}_1(\mathbf{r})-\Theta^{i^{nm}}(\mathbf{r}),\quad \mathbf{r}\in\Xi\cap\tilde{\Gamma}_2,\\&\boldsymbol{\xi}^{nm}(\mathbf{r})=-\boldsymbol{\xi}^{i^{nm}}(\mathbf{r}),\ \lambda^{nm}(\mathbf{r})=-\lambda^{i^{nm}}(\mathbf{r}),\quad \mathbf{r}\in\Xi\cap\tilde{\Gamma}_2.\end{aligned}$$

These are $8(n-1)$ equations.

• Evaluate the boundary conditions for at $z=1$ for the nodes r_i, $i=1,\cdots,n-1$,

$$
\begin{aligned}
&u_z^{nm}(\mathbf{r})=-u_z^{i^{nm}}(\mathbf{r}),\ \ \partial_z u_r^{nm}(\mathbf{r})=-\partial_z u_r^{i^{nm}}(\mathbf{r}),\ \ \partial_z u_\phi^{nm}(\mathbf{r})=-\partial_z u_\phi^{i^{nm}}(\mathbf{r}),\\
&2\partial_z\Theta^{nm}(\mathbf{r})+B\Theta^{nm}(\mathbf{r})-Bh^n(\mathbf{r})=-2\partial_z\Theta^{i^{nm}}(\mathbf{r})-B\Theta^{i^{nm}}(\mathbf{r})-Bh^{i^n}(\mathbf{r}),\\
&\xi_z^{nm}(\mathbf{r})=-\xi_z^{i^{nm}}(\mathbf{r}),\ \ \partial_z\xi_r^{nm}(\mathbf{r})=-\partial_z\xi_r^{i^{nm}}(\mathbf{r}),\ \ \partial_z\xi_\phi^{nm}(\mathbf{r})=-\partial_z\xi_\phi^{i^{nm}}(\mathbf{r}),\\
&2\partial_z\lambda^{nm}(\mathbf{r})+B\lambda^{nm}(\mathbf{r})=-2\partial_z\lambda^{i^{nm}}(\mathbf{r})-B\lambda^{i^{nm}}(\mathbf{r}),\\
&B\lambda^{nm}(\mathbf{r})-\eta h^n(\mathbf{r})=-B\lambda^{i^{nm}}(\mathbf{r})-\eta h^{i^n}(\mathbf{r}),\quad \mathbf{r}\in\Xi\cap\tilde\Gamma_1.
\end{aligned}
$$

Consequently, $8(n-1)+(n+1)$ new equations are obtained.

• Regarding to the boundary conditions and as the problem has been solved in primitive variables formulation by expanding the fields with Chebyshev polynomials, the problem of spurious modes for pressure arises [4, 7]. We have solved it by using the method proposed in [11], which requires additional boundary conditions. These conditions include the evaluation of the normal projections of the Navier-Stokes equations on $\tilde\Gamma_1$ and $\tilde\Gamma_0$ and the continuity equation on $\tilde\Gamma_2$. The same problem of the existence of spurious modes arises for the adjoint pressure field π. An equivalent methodology has been applied for the adjoint pressure field, i.e., the evaluation of the normal projections of the adjoint Navier-Stokes equations on $\tilde\Gamma_1$ and $\tilde\Gamma_0$ and the corresponding adjoint continuity equation on $\tilde\Gamma_2$. Then the following boundary conditions are added. The continuity equation is evaluated at $z=-1$ for the nodes r_i, $i=1,\cdots,n-1$,

$$
\begin{aligned}
&Gu_r^{nm}(\mathbf{r})+A\partial_r u_r^{nm}(\mathbf{r})+2\partial_z u_z^{nm}(\mathbf{r})\\
&=-Gu_r^{i^{nm}}(\mathbf{r})-A\partial_r u_r^{i^{nm}}(\mathbf{r})-2\partial_z u_z^{i^{nm}}(\mathbf{r}),\quad \mathbf{r}\in\Xi\cap\tilde\Gamma_2.
\end{aligned}
$$

The continuity equation for the auxiliary field ξ can be treated similarly. The normal component of the momentum equation is evaluated at $z=1$ for the nodes r_i, $i=1,\cdots,n$,

$$
\begin{aligned}
&\mathrm{Pr}^{-1}(Au_r^{i^{nm}}\partial_r u_z^{nm}+Au_r^{nm}\partial_r u_z^{i^{nm}}+2u_z^{i^{nm}}\partial_z u_z^{nm}+2u_z^{nm}\partial_z u_z^{i^{nm}})(\mathbf{r})\\
&\quad+2\partial_z p^{nm}(\mathbf{r})-\Delta_b u_z^{nm}(\mathbf{r})-R\Theta^{nm}(\mathbf{r})=-\mathrm{Pr}^{-1}(Au_r^{i^{nm}}\partial_r u_z^{i^{nm}}+2u_z^{i^{nm}}\partial_z u_z^{i^{nm}})(\mathbf{r})\\
&\quad-2\partial_z p^{i^{nm}}(\mathbf{r})+\Delta_b u_z^{i^{nm}}(\mathbf{r})+R\Theta^{i^{nm}}(\mathbf{r}),\quad \mathbf{r}\in(\Xi\cap\tilde\Gamma_1)\cup\{(r_n,1)\}.
\end{aligned}
$$

The momentum equation for the auxiliary field ξ can be handled in a similar way. The normal component of the momentum equation is evaluated at $r=1$ for the nodes z_j, $j=0,\cdots,m-1$,

$$
\begin{aligned}
&\mathrm{Pr}^{-1}(Au_r^{i^{nm}}\partial u_r^{nm}+Au_r^{nm}\partial u_r^{i^{nm}}+2u_z^{i^{nm}}\partial_z u_r^{nm}+2u_z^{nm}\partial_z u_r^{i^{nm}}-2Gu_\phi^{i^{nm}}u_\phi^{nm})(\mathbf{r})\\
&\quad+A\partial_r p^{nm}(\mathbf{r})-\Delta_b u_r^{nm}(\mathbf{r})+G^2u_r^{nm}(\mathbf{r})=-\mathrm{Pr}^{-1}(Au_r^{i^{nm}}\partial u_r^{i^{nm}}+2u_z^{i^{nm}}\partial_z u_r^{i^{nm}}\\
&\quad-G(u_\phi^{i^{nm}})^2)(\mathbf{r})-A\partial_r p^{i^{nm}}(\mathbf{r})+\Delta_b u_r^{i^{nm}}(\mathbf{r})-G^2u_r^{i^{nm}}(\mathbf{r}),\quad \mathbf{r}\in(\Xi\cap\tilde\Gamma_0)/\{1,z_m\}.
\end{aligned}
$$

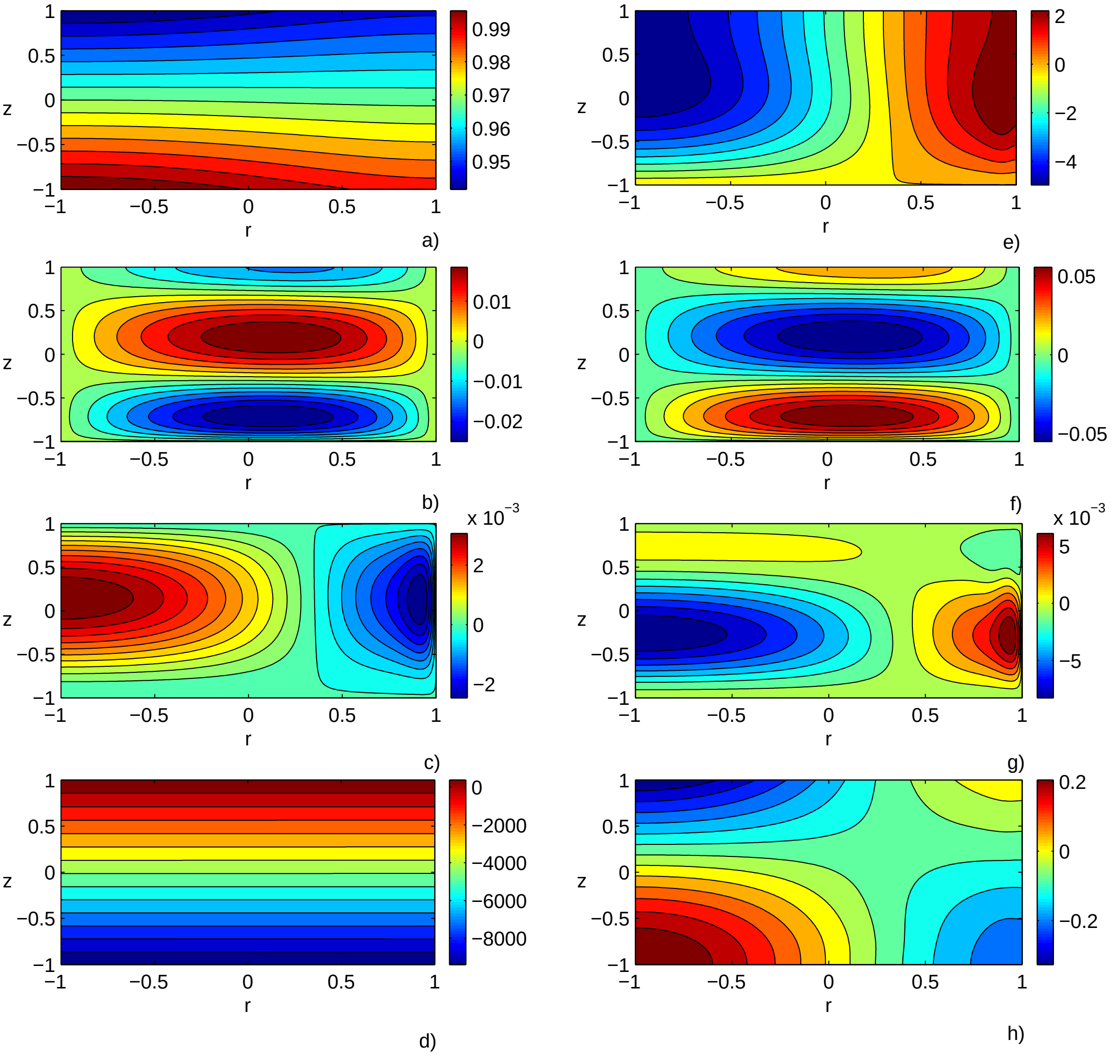

Figure 3: Contour plots for the fields of a controlled basic state and adjoint state; a) Θ; b) u_r; c) u_z; d) p; e) λ; f) ξ_r; g) ξ_z; h) π. The parameters are $B=0.05$, $\gamma=10$, $\mathrm{Pr}=0.4$, $\mathrm{R}=14736$, $\delta=0.01$, $\beta=5$ and $\eta=1$.

The continuity equation for the auxiliary field ξ can be handled in a similar way. Then, additional $2((n-1)+n+m)$ equations are obtained.

- With these rules we get a matrix of order $P\times P$, where

$$
\begin{aligned}
P&=10(n-1)(m-1)+18(m+1)+18(n-1)+n+1+2n+2m\\
&=10(n+1)(m+1)+(n+1).
\end{aligned}
$$

However this matrix associated with the linear algebraic system is singular, due to the fact that pressure with the imposed conditions is defined up to a constant. To fix this

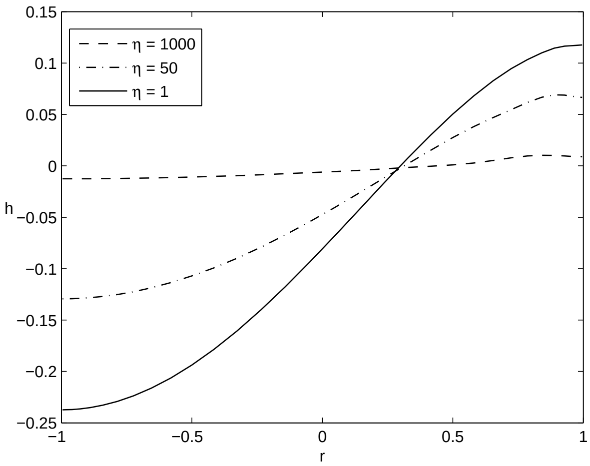

Figure 4: Control functions h at different values of η. The rest of the parameters are $B=0.05$, $\gamma=10$, $\mathrm{Pr}=0.4$, $\mathrm{R}=11500$, $\delta=0.01$, $\beta=5$.

constant a boundary condition at node $(1,z_4)$ is replaced by a Dirichlet condition for pressure p and the adjoint π (i.e., $p=0$ and $\pi=0$). In this way, a linear system of the form $AX=B$ is obtained, where X is a vector containing P unknowns and A is a full rank matrix of order $P\times P$. This can be easily solved with standard routines. In particular we have used a direct Gauss method in MATLAB. So, starting with $U^{0^{nm}}$, the iterative procedure is applied until the stop criterion is satisfied:

$$\|U^{nm}\|_2=\left\|U^{i+1^{nm}}-U^{i^{nm}}\right\|_2\leq 10^{-9}.$$

Numerical solutions for the different fields can be seen in Figs. 3 and 4. Fig. 3 shows contour plots for the fields of a controlled basic state (Figs. 3(a)-(d)) and the corresponding contour plots for the adjoint fields (Figs. 3(e)-(h)). Fig. 4 shows the profile of the control function h at different values of η. Note that there is a direct relationship between the regular Gaussian heating profile at the bottom Θ_1 and the profile of the control function h: they have opposite gradients.

3.2.4 Linear stability analysis

The linear stability analysis of the controlled basic states can reveal interesting results on controlling the instabilities developed for the uncontrolled states [19]. In this section, the numerical method used to perform this study is detailed. The stability of the basic state is studied by perturbating it with a vector field depending on the r, ϕ and z coordinates, in a fully 3D analysis:

$$w(r,\phi,z)=w^b(r,z)+\bar{w}_r(r,z)e^{ik\phi+\lambda t}, \tag{3.21}$$

where w refers to the unknown fields u_r, u_ϕ, u_z, p and Θ. Here the superscript b indicates the corresponding quantity in the basic state and the bar refers to the perturbation.

Fourier modes along the angular coordinate ϕ, satisfy the periodic boundary conditions as long as k is an integer. Expression (3.21) are substituted into the basic equations (3.15a)-(3.15e) and boundary and regularity conditions (3.16) and (3.14). Regularity conditions (3.14) depend now on the wavenumber k [11]:

$$u_r = u_\phi = \frac{\partial u_z}{\partial r} = \frac{\partial \Theta}{\partial r} = \frac{\partial p}{\partial r} = 0, \quad \text{for } k=0, \tag{3.22}$$

$$u_r + i u_\phi = u_z = \Theta = p = 0, \quad \text{for } k=1, \tag{3.23}$$

$$u_r = u_\phi = u_z = \Theta = p = 0, \quad \text{for } k \neq 0,1. \tag{3.24}$$

Linearizing the resulting system we get a generalized eigenvalue problem in λ. The eigenvalue problem is discretized following the Chebyshev collocation method explained in the previous section by expanding perturbations $\bar{u}_r$, $\bar{u}_\phi$, $\bar{u}_z$, $\overline{\Theta}$ and $\overline{p}$ in a truncated series of orthonormal Chebyshev polynomials, i.e.,

$$\bar{u}_r = \sum_{l=0}^{n} \sum_{s=0}^{m} a_{ls} T_l(r) T_s(z), \tag{3.25}$$

and similarly for $\bar{u}_\phi$, $\bar{u}_z$, $\bar{\Theta}$ and $\bar{p}$. There are $P = 5\times(n+1)\times(m+1)$ unknowns which are determined by the collocation method explained in [18]. The eigenvalue problem is then transformed into its discrete form

$$Aw = \lambda Bw, \tag{3.26}$$

where $w = (a_{ls}, b_{ls}, c_{ls}, d_{ls}, e_{ls})^T$ is a vector which contains P unknowns and A and B are $P\times P$ matrices. If we define

$$\lambda_{\max} = \max_{\mathrm{i}=1,\cdots,\bar{\mathrm{r}}} \{Re(\lambda_i)\},$$

the stationary solution passes from stable to unstable state when R takes a certain critical value R_c^k (the one for which $\lambda_{\max}(k, \mathrm{R}_c^k) = 0$). Define next the pair (k_c, R_c) by the relation

$$\mathrm{R}_c = \min_{k\in I} \left\{ \mathrm{R}_c^k \right\},$$

where $I \subset \mathbb{N}$ is a certain interval of natural numbers which will be usually contained in $I = [0,30]$. The bifurcation occurs exactly for (k_c, R_c). If the eigenvalue associated to $\lambda_{\max}(k_c, \mathrm{R}_c)$ is complex the bifurcation is oscillatory, if it is real the instability is stationary. The algorithm to compute efficiently $\lambda_{\max}$ is widely explained in [20].

4 Numerical results

A test on the convergence of the numerical method is carried out by comparing the differences in the value of the critical Rayleigh number for different orders of expansions in Chebyshev polynomials. These values are shown in Table 1 for $B=0.05$, $\gamma=10$, $\delta=0.01$, $\beta=5$ and $\eta=0.01$ for several consecutive expansions varying the number of polynomials

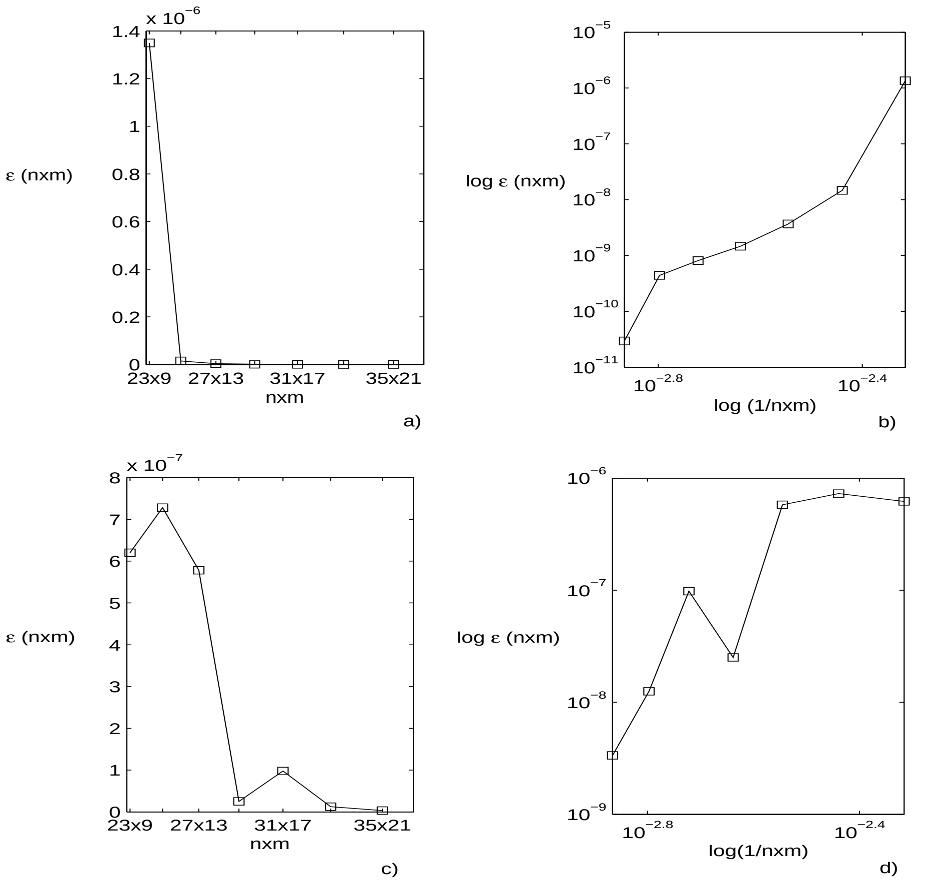

Figure 5: a) Relative differences in R_c between order expansions (ε) as a function of the order expansion for $\eta=100$; b) logarithmic representation of figure a); c) ε as a function of the order expansion for $\eta=1$; d) logarithmic representation of figure c). The rest of the parameters are $B=0.05,\gamma=10,\mathrm{Pr}=0.4,\delta=0.01$ and $\beta=5$.

taken in the r (n) and z (m) coordinates. As it can be deduced from Table 1 there is no significant difference in the value of the R_c when m is increased. To get reliable results in every case we have considered expansion 39×13 in our computations. Regarding to convergence we have observed that there is a dependence of the rate of convergence on the value of parameter η. In Figs. 5 and 6 it is shown the relative differences in R_c number between consecutive expansions:

$$\varepsilon(n\times m)=\left|\mathrm{R}_{cn\times m}-\mathrm{R}_{c(n-2)\times(m-2)}\right|/\mathrm{R}_{cn\times m},$$

for $B=0.05$, $\gamma=10$, $\delta=0.01$ and $\beta=5$. This is represented for four different values of η, $\eta=100$, 1, 0.01, 0.0002 (Figs. 5a, 5c, 6a and 6c). As the order increases the differences tend to zero but the rate of convergence decreases with η. A logarithmic representation of the previous figures is shown in figures (Figs. 5b, 5d, 6b and 6d). The gradient of the line

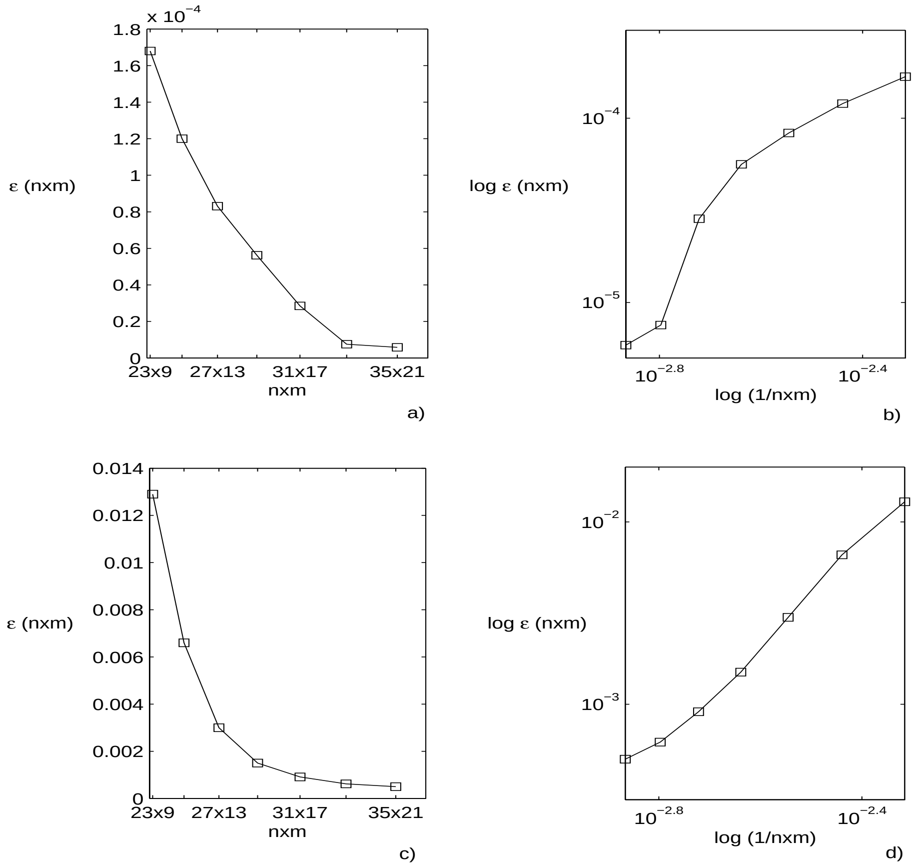

Figure 6: a) Relative differences in R_c between order expansions (ε) as a function of the order expansion for $\eta=0.01$; b) logarithmic representation of figure a); c) ε as a function of the order expansion for $\eta=0.0002$; d) logarithmic representation of figure c). The rest of the parameters are $B=0.05,\gamma=10,\mathrm{Pr}=0.4,\delta=0.01$ and $\beta=5$.

corresponds to the order which the method acts with in each case. This gradient is nearly 8.2 for $\eta=100$ and decreases till 2.5 for $\eta=0.0002$.

Table 1: Critical Rayleigh number for the controlled solutions at $B=0.05$, $\gamma=10,\mathrm{Pr}=0.4$, $\delta=0.01$ and $\beta=5$, at $\eta=0.01$ for different order expansions in n and m.

	$m=9$	$m=11$	$m=13$	$m=15$	$m=17$
$n=23$	11902.32	11902.39	11902.40	11902.40	11902.41
$n=27$	11905.86	11905.78	11905.77	11905.77	11905.77
$n=31$	11907.47	11907.44	11907.42	11907.42	11907.42
$n=37$	11907.73	11907.79	11907.79	11907.79	11907.79
$n=39$	11907.65	11907.68	11907.68	11907.68	11907.68
$n=41$	11907.59	11907.60	11907.60	11907.60	11907.60

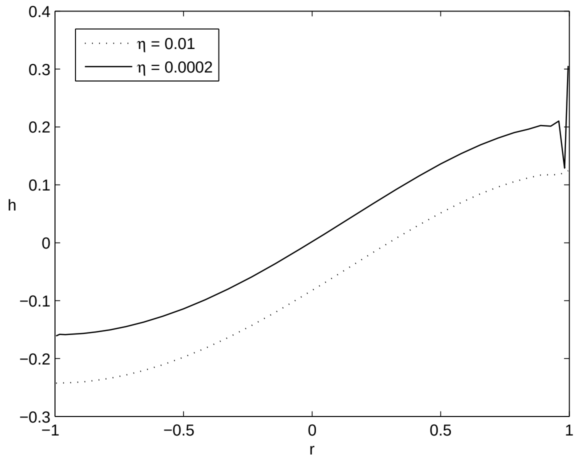

Figure 7: Control functions h at two small different values of η. The rest of the parameters are $B=0.05$, $\gamma=10$, $\mathrm{Pr}=0.4$, $\mathrm{R}=11500$, $\delta=0.01$, $\beta=5$.

This dependence on η can arise from the fact that some singularities in the controlled state solutions are found as η is increasingly reduced. Fig. 7 shows the profile of the control function h for two different small values of η. Observe the irregular shape near $r=1$. This can be due to the smallness of η, because as η decreases the optimal control problem tends to be ill posed as in the limit $\eta=0$ the problem makes no sense. However, once the control problem is solved, regularized h profiles can be considered directly in the problem (2.1)-(2.8). The regularization is solved by avoiding the boundary layer on $r=1$ similarly to $r=-1$. The basic states obtained have the same reduction in enstrophy and identical linear stability properties than the controlled states without regularization. The convergence properties of the method remain. So the singularities are irrelevant in the problem as a regularized control function produces the same results.

5 Concluding remarks

In this work a Chebyshev collocation method has been used for solving numerically an optimal boundary control problem in a thermoconvective fluid flow. In the computer implementation several procedures have been developed to deal with some troubles. A Newton method is used for the nonlinear terms. As the problem is treated in the primitive variable formulation additional boundary conditions for the pressure and the auxiliary pressure fields are required to avoid spurious modes. Also regularity conditions are needed for the treatment of the problem in cylindrical coordinates. A dependence of the convergence of the method on the penalizing parameter that appears in the functional cost is observed. As this parameter approaches zero some singular behaviour in the control function is observed and the order of the method decreases. These singularities are irrelevant in the problem as a regularized control function produces the same results.

Acknowledgments

This work was partially supported by the Research Grants MCYT (Spanish Government) MTM2006-14843-C02-01 and CCYT (JC Castilla-La Mancha) PAC-05-005, which include ERDF funds.

References

[1] F. Abergel and E. Casas, Some optimal control problems of multistate equations appearing in fluid mechanics, RAIRO Model. Math. Anal. Numer., 27 (1993), 223-247.
[2] F. Abergel and R. Teman, On some control problems in fluid mechanics, Theoret. Comput. Fluid Dynamics, 1 (1990), 303-325.
[3] H. Bénard, Les tourbillons cellulaires dans une nappe liquide, Rev. Gén. Sci. Pures Appl., 11 (1900), 1261.
[4] C. Bernardi and Y. Maday, Approximations Spectrales de Problemes aux Limites Elliptiques, Springer-Verlag, Paris, 1992.
[5] C. Bernardi, C. Canuto and Y. Maday, Generalized inf-sup conditions for Chebyshev spectral approximation of the Stokes problem, SIAM J. Numer. Anal., 25 (1988), 1237-1271.
[6] C. Bernardi and Y. Maday, Properties of some weighted Sobolev spaces and applications to spectral approximations, SIAM J. Numer. Anal., 26(4) (1989), 769-829.
[7] C. Canuto, M. Y. Hussaini, A. Quarteroni and T. A. Zang, Spectral Methods in Fluid Dynamics, Springer-Verlag, Berlin, 1988.
[8] M. Desai and K. Ito, Optimal control of Navier-Stokes equations, SIAM J. Optim. Control, 32 (1994), 1428-1446.
[9] H. O. Fattorini and S. S. Sritharan, Existence of optimal controls for viscous flow problems, Proc. Roy. Soc. London Ser. A, 439 (1992), 81-102.
[10] M. Gunzburger, L. Hou and T. Svobodney, Analysis and finite elements approximation of optimal control problems for the stationary Navier-Stokes equations with Dirichlet controls, RAIRO Model. Math. Anal. Numer., 25 (1991), 123-151.
[11] H. Herrero and A. M. Mancho, On pressure boundary conditions for thermoconvective problems, Int. J. Numer. Meth. Fluids, 39 (2002), 391-402.
[12] L. S. Hou and S. S. Ravindran, Penalty methods for numerical approximations of optimal boundary flow control problems, Int. J. Comput. Fluid D, 11(1-2) (1998), 157-167.
[13] S. Hoyas, H. Herrero and A. M. Mancho, Thermal convection in a cylindrical annulus heated laterally, J. Phys. A: Math and Gen., 35 (2002), 4067-4083.
[14] S. Hoyas, A. M. Mancho, H. Herrero, N. Garnier and A. Chiffaudel, Bénard-Marangoni convection in a differentially heated cylindrical cavity, Phys. Fluids, 17 (2005), 054104.
[15] K. Ito and S. S. Ravindran, Optimal control of thermally convected fluid flows, SIAM J. Sci. Comput., 19 (1998), 1847-1869.
[16] A. M. Mancho and H. Herrero, Instabilities in a laterally heated liquid layer, Phys. Fluids, 12 (1998), 1044-1051.
[17] I. Mercader, M. Net and A. Falques, Spectral methods for high order equations, Comp. Methods Appl. Mech. Engrg., 91 (1991), 1245-1251.
[18] M. C. Navarro, A. M. Mancho and H. Herrero, Instabilities in buoyant flows under localised heating, Chaos, 17 (2007), 023105 1-10.

[19] M. C. Navarro and H. Herrero, Effects of optimal control over thermoconvective patterns, Phys. Rev. E, 75 (2007), 067203 1-4.

[20] M. C. Navarro, H. Herrero, A. M. Mancho and A. Wathen, Efficient solution of a generalized eigenvalue problem arising in a thermoconvective instability, Commun. Comput. Phys., 3 (2008), 308-329.

[21] T. Okutani, H. Nagai and Y. Nakata, Synthesis of homogeneous materials by splat solidification in short-duration microgravity, Key Eng. Mat., 264-268: 761-764, 2004.

[22] N. Postacioglu, P. Kapadia and J. Dowen, A theoretical model of thermocapillary flows in laser welding, J. Phys. D: Appl. Phys., 24 (1991), 15-20.

[23] Lord Rayleigh, On convective currents in a horizontal layer of fluid when the temperature is on the under side, Phil. Mag., 32 (1916), 529-46.

[24] S. Sritharan, Dynamic programming of the Navier-Stokes equations, System Control Lett., 16 (1991), 229-307.